

Effect of Operating Conditions on the Ceramic Particles Drying Process by Superheated Steam in the Packed Bed Dryer

Thi Thu Hang Tran¹, Kieu Hiep Le^{1*}, Thi Thu Huong Tran²

¹Hanoi University of Science and Technology, No.1 Dai Co Viet str., Hai Ba Trung dist., Hanoi, Viet Nam

²University of Economics - Technology for Industries, 456 Minh Khai str., Hai Ba Trung dist., Hanoi, Viet Nam

Received: April 05, 2020; Accepted: November 12, 2020

Abstract

A novel model of ceramic particle drying by superheated steam in the packed bed dryer is applied to examine the effects of operating conditions on the drying process. It is shown that the drying kinetic has two drying stages: the evaporation flux firstly increases to the maximum value while particle temperature is remained as saturation temperature, then the evaporation flux decreases to the zero, and particle temperature rises to the equilibrium temperature. Results also illustrate that the drying process is faster at the thinner bed layer, smaller particle diameter, and higher initial vapor velocity and temperature.

Keywords: Superheated steam drying, ceramic drying, packed bed

1. Introduction

Super-heated steam drying (SSD) has been applied in many industrial fields such as chemical engineering, food engineering, coal, etc. because it is cheaper and more friendly than the hot air drying (HAD) technique [1]. In SSD, super-heated steam is used as a drying agent so the exhausted agent can be reused or recycled. Thus, SSD gives higher energy efficiency and lower carbon dioxide emission. At temperature above the inversion temperature, the drying rate in SSD is higher than that in HAD. Additionally, due to no oxygen, the quality of product dried in SSD is better than that in HAD [2,3]. In terms of dryer system, a packed bed dryer is one of the common techniques because it is a simple operation and low mechanical damage to the material [4].

The study of individual particle drying kinetic has been concerned as a solution to complex transports occurring inside the packed bed. There have been several models that can be categorized into empirical models and theoretical models. The empirical models are easy to implement in the macro-scale model [5,6]. However, these were obtained from several sets of the experiment so the application ability is limited in the experiment condition. Regarding theoretical models, the partial distributions of temperature and moisture content in the particle often are considered [7–9]. In these theoretical models, moisture content gradient is driving force of

only water or both liquid water and water vapor transport inside particle. In the previous own work [10], a novel model was applied and validated for the multiscale model of ceramic particles drying in the packed bed dryer by super-heated steam. In this work, Reaction Engineering Approach (REA) applied for drying is analogy with chemical reaction kinetics. This model has the advantage that the model parameters are determined from one set of experimental data, but it was successful validated for other conditions. After that, the macro-scale model of super-heated steam packed bed drying is built by volume averaging technique.

In this work, the built model is simulated for a range of operating conditions to examines the effects of drying conditions on the drying process of ceramic particles in a packed bed dryer. From this, advice will be given to increase the energy efficiency of the system.

2. Mathematical model

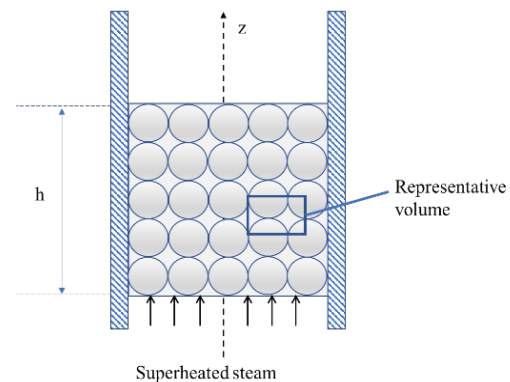


Fig. 1. Geometry of packed bed

*Corresponding author: Tel.: (+84) 971381294
Email: hiep.lekieu@hust.edu.vn

The packed bed dryer is composed of uniform spherical ceramic particles and a super-heated steam phase as Fig.1. It is assumed that the particle porosity is uniform, and flow is plug flow, viscous dissipation and compression are negligible, vapor evaporated from particles is much smaller than the inlet steam flow, the bed is isotropic and homogeneous porous media.

The mathematical model is developed and verified in Ref. [10] in detail. In this paper, the model is only recalled briefly in following sections.

2.1. Heat and mass transfer

Heat and mass conservation equations were developed based on volume averaging technique [9,11]. For the fluid phase, the temperature change is the result of enthalpy flow from the vapor phase, heat flow from evaporated vapor, convective heat transfer from drying particles as Eq. 1:

$$\begin{aligned} \psi c_{p,v} \rho_v \frac{\partial T_v}{\partial t} + c_{p,v} \rho_v v_v \frac{\partial T_v}{\partial z} = \frac{\partial}{\partial z} \left(\lambda_{v,eff} \frac{\partial T_v}{\partial z} \right) \quad (1) \\ -\dot{m}_v A_v c_{p,v} (T_v - T_s) - \alpha A_v (T_v - T_s) \end{aligned}$$

where, ψ is bed porosity; $c_{p,v}$ [J/kgK], ρ_v [kg/m³], v_v [m/s], $\lambda_{v,eff}$ [W/mK] are heat capacity, density, velocity, effective heat conductivity of vapor, respectively; T_v and T_s [K] are vapor temperature and solid temperature, respectively. A_v [m²/m³] is specific area. α [W/m²K] is the heat transfer coefficient. The evaporation flux \dot{m}_v [kg/m²s] is calculated as in Section 2.3.

The enthalpy flow change and mass conservation of solid phase are expressed as:

$$(1-\psi) \left\langle c_{p,s,eff} \rho_{s,eff} \right\rangle \frac{\partial T_s}{\partial t} = \frac{\partial}{\partial z} \left(\lambda_{s,eff} \frac{\partial T_s}{\partial z} \right) \quad (2) \\ -\dot{m}_v A_v \Delta h_{evp} + \alpha A_v (T_v - T_s)$$

$$(1-\psi) \frac{\partial \rho_{s,eff}}{\partial t} = -\dot{m}_v A_v \quad (3)$$

in which $c_{p,s,eff}$ [J/kgK], $\rho_{s,eff}$ [kg/m³], $\lambda_{s,eff}$ [W/mK] and T_s [K] are effective heat capacity, effective density, and effective heat conductivity, temperature of solid phase, respectively. Δh_{evp} [J/kg] is the evaporation latent heat. These effective physical properties in the above equations of the packed bed are calculated from:

$$\rho_{s,eff} = \rho_s (1 + X) \quad (4)$$

$$\left\langle c_{p,s,eff} \rho_{s,eff} \right\rangle = \rho_s (c_{p,s} + X c_{p,l}) \quad (5)$$

$$\lambda_{s,eff} = (1-\psi) \left(\lambda_s \frac{m_s}{V} + \lambda_l \frac{m_l}{V} \right) = \quad (6) \\ (1-\psi) (\lambda_s \rho_s + \lambda_l \rho_l X)$$

$$\lambda_{f,eff} = \psi \lambda_v \quad (7)$$

in which, X is moisture content (kg water / kg dry basis) of the bed.

2.2. Thermal boundary conditions

The temperature of vapor is assumed as constant at the packed bed inlet:

$$\frac{\partial T_v}{\partial t} = 0 \quad (8)$$

Particle temperature at inlet is calculated by:

$$(1-\psi) \left\langle c_{p,s,eff} \rho_{s,eff} \right\rangle \frac{\partial T_s}{\partial t} = \frac{\partial}{\partial z} \left(\lambda_{s,eff} \frac{\partial T_s}{\partial z} \right) \Big|_{z=0} \quad (9) \\ -\dot{m}_v A_v \Delta h_{evp} + \alpha A_v (T_v - T_s)$$

At the outlet, energy conservation for particles and vapor is calculated as:

$$(1-\psi) \left\langle c_{p,s,eff} \rho_{s,eff} \right\rangle \frac{\partial T_s}{\partial t} = \frac{\partial}{\partial z} \left(\lambda_{s,eff} \frac{\partial T_s}{\partial z} \right) \Big|_{z=h} \quad (10) \\ -\dot{m}_v A_v \Delta h_{evp} + \alpha A_v (T_v - T_s)$$

In the above equations, evaporation flux \dot{m}_v is determined by Reaction Engineering Approach developed for super-heated steam drying.

2.3. Drying kinetic

Drying dynamic is the difference of vapor density at the particle surface and bulk vapor $\rho_{v,surf}$, $\rho_{v,b}$ (kg vapor/m³) as

$$\dot{m}_v = -\beta (\rho_{v,surf} - \rho_{v,b}) \quad (11)$$

where β (m/s) is the mass transfer coefficient. The relationship between vapor density at the particle surface and at the pure water droplet surface is:

$$\rho_{v,surf} = \exp \left(\frac{-\Delta E_v}{RT_s} \right) \rho_{v,sat} (T_s) \quad (12)$$

where the activation energy ΔE_v of the particle and the equilibrium activation energy $\Delta E_{v,eq}$ is determined by experimental data [10]:

$$\frac{\Delta E_v}{\Delta E_{v,eq}} = \frac{7.42 \times 10^{-3}}{(X - X_{eq}) + 7.63 \times 10^{-3}} \quad (13)$$

$$\Delta E_{v,eq} = RT_{v,b} \ln \left(\frac{P_{v,b}}{P_{v,sat}(T_{v,b})} \right) \quad (14)$$

Heat and mass transfer coefficients between particle and vapor are calculated as

$$Nu = 2 + 0.616 Re^{0.52} Pr^{\frac{1}{3}} \quad (15)$$

$$Sh = 0.144 + 0.579 Re^{0.5} Sc^{1/3} \quad (16)$$

3. Results and discussion

As mentioned, the mathematical model was successful validated by a comparison between predictive and experimental data in terms of drying rate and outlet vapor temperature as Fig.2 and Fig.3 as shown in [11].

Here, the model is applied to examine the effect of particle diameter d [m], bed height h [m], inlet vapor temperature $T_{v,in}$ [°C], and inlet vapor velocity v_m [m/s] on the ceramic particle drying. In each analysis, there is only one variable, other variables are kept constant.

3.1. Effect of particle diameter

Evolutions of evaporation flux, vapor temperature, and solid temperature at the packed bed outlet over time are presented in Fig.4-6 corresponding with different particle diameters. It is observed in Fig.4 that, m_v increases when particle diameter reduces resulting in the shorter drying time. The reason is that the faster heat and mass transfers occurs in drying process of smaller particles. In these cases, the evaporation flux increases to the maximum

value then it decreases gradually. This trend is different from the drying kinetic of single particle which experiences the constant drying period followed by falling drying period. The increase of drying flux in the first period can be explained by the change of vapor temperature flowing through the bed as Fig.6. The particle water content reduces which gives the decrease of vapor density on the particle surface, but the heat and mass transfer coefficient rise due to the accession of thermal conductivity and reduction of viscosity of vapor at higher vapor temperature. This first drying period corresponds with the constant solid temperature stage (Fig.5). However, after a certain period, the heat and mass transfer from vapor are not enough to remain the high evaporation speed and constant solid temperature, the evaporation flux goes to the falling period. In this, evaporation flux drops to zero at the end of the drying process while the solid temperature increases to the equilibrium temperature (Fig.5). This is because of the increase in the evaporation energy barrier corresponding with the reduction of particle moisture content.

It can be observed in Fig.5 that the vapor temperature at bigger particle is higher than that at smaller particle due to the slower drying speed of big particle. However, the vapor at big particle drying bed changes slower to the equilibrium temperature (for $d = 0.015$ m, vapor temperature reaches the m_v equilibrium temperature after 800 s while for $d = 0.005$ m, this period is about 400 s). The low heat and mass transfer coefficients are also the reason of this comparison.

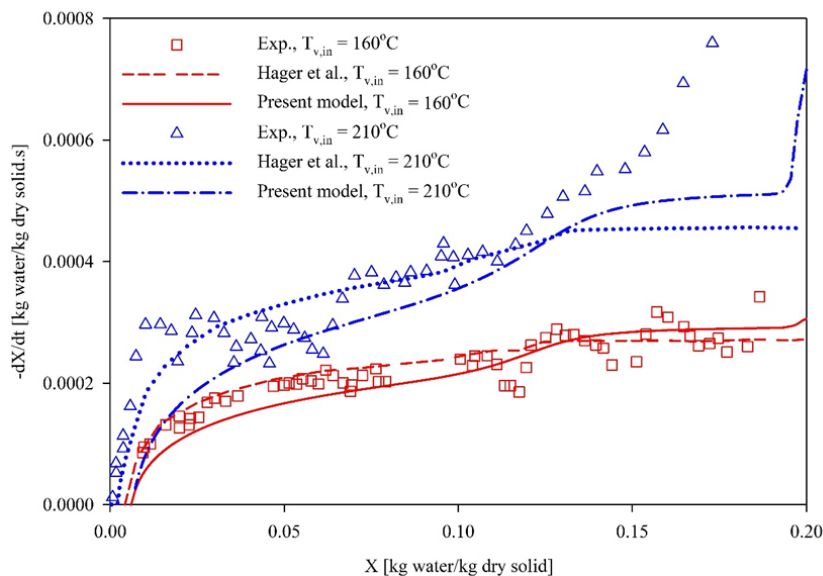


Fig. 2. Comparisons of drying rates obtained from simulations and measurements.

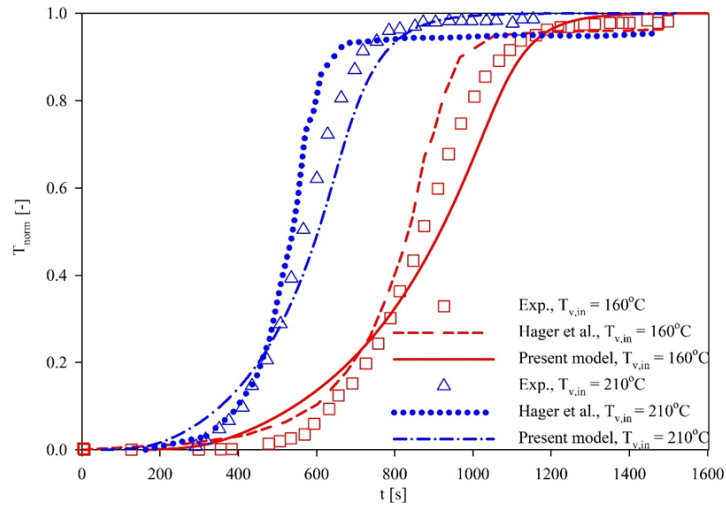


Fig. 3. Comparisons of outlet vapor temperature obtained from experiments and simulations.

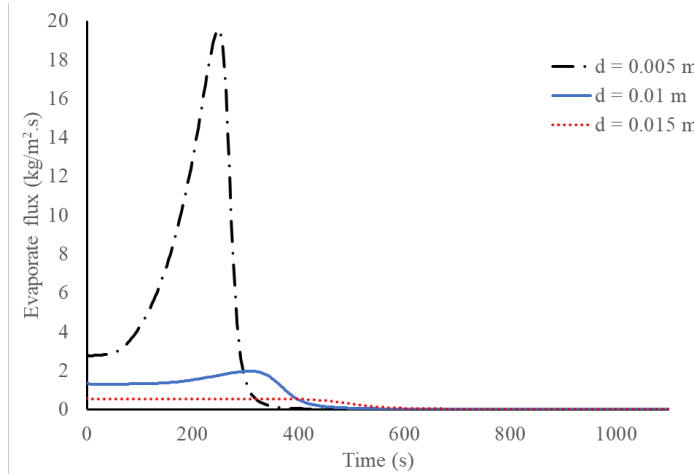


Fig. 4. Evaporation flux at the middle of the bed at $T_{v,in} = 210\text{ }^{\circ}\text{C}$, $v_{in} = 1.5\text{ m/s}$, $X_{w,in} = 0.2\text{ kg/kg}$, $h = 0.1\text{ m}$

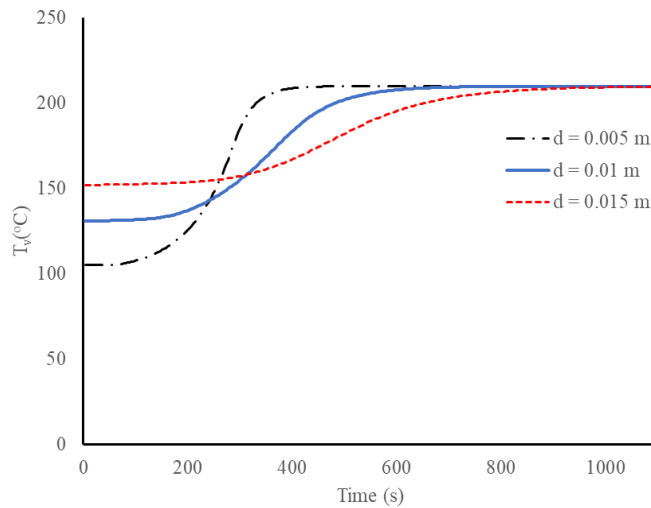


Fig. 5. Vapor temperature, T_v at the middle of the bed at $T_{v,in} = 210\text{ }^{\circ}\text{C}$, $v_{in} = 1.5\text{ m/s}$, $X_{w,in} = 0.2\text{ kg/kg}$, $h = 0.1\text{ m}$

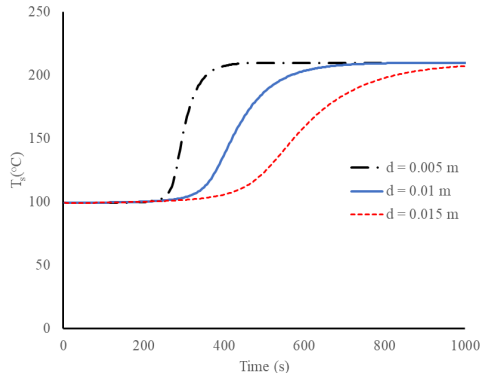


Fig. 6. Particle temperature, T_s at the middle of the bed at $T_{v,in} = 210$ °C, $v_{in} = 1.5$ m/s, $X_{w,in} = 0.2$ kg/kg, $h = 0.1$ m

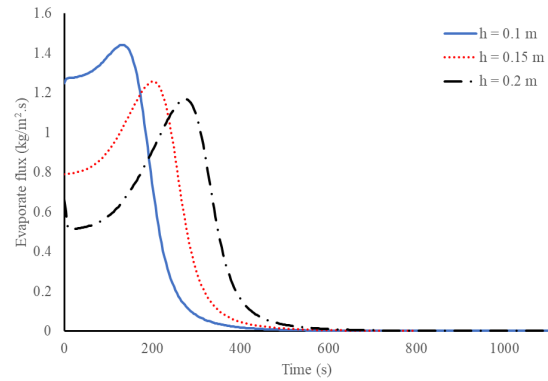


Fig. 7. Evaporation flux, m_v at the middle of the bed at $T_{v,in} = 210$ °C, $v_{in} = 1.5$ m/s, $X_{w,in} = 0.2$ kg/kg, $d = 0.01$ m

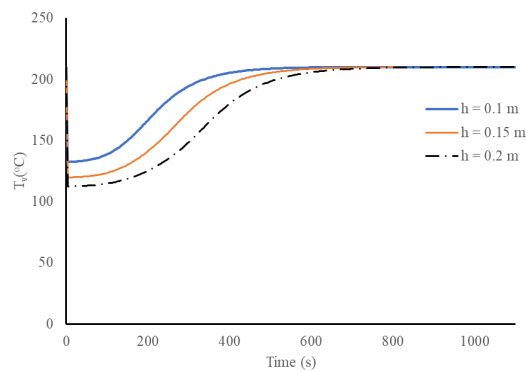


Fig. 8. Vapor temperature, T_v at the middle of the bed at $T_{v,in} = 210$ °C, $v_{in} = 1.5$ m/s, $X_{w,in} = 0.2$ kg/kg, $d = 0.01$ m

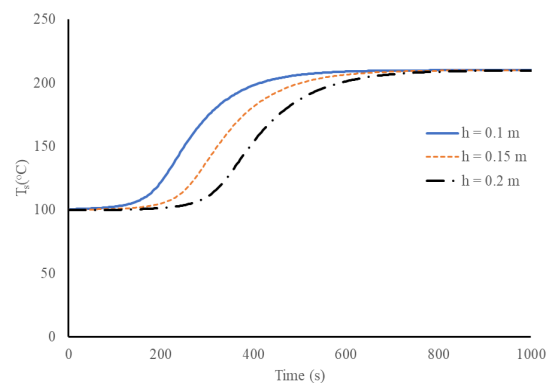


Fig. 9. Particle temperature, T_s at the middle of the bed at $T_{v,in} = 210$ °C, $v_{in} = 1.5$ m/s, $X_{w,in} = 0.2$ kg/kg, $d = 0.01$ m

Regarding Fig.6, during the first drying period, particle temperature remains constant because the heat flow is enough for only evaporation. After the maximum point of evaporation flux, the solid particle starts to increase gradually to the vapor temperature at the end. Besides, smaller particle temperature reaches the maximum temperature earlier than the bigger particle; like the vapor temperature change, the faster heat transfer of smaller particles is the reason for this observation.

3.2. Effect of bed height

Comparisons of drying of middle bed at different bed heights are presented in Fig.7-9. It can be seen in Fig.7 that the thinner particle layer gives faster drying and shorter drying time. The reason is that at the thin particle layer, the vapor flows through the shorter distance so the vapor enthalpy used for heat and mass transfer is lower resulting in the higher vapor temperature (Fig.8).

In case of thin bed particle temperature remains constant corresponding with the increase of evaporation flux for a shorter time. The particle

temperature and vapor temperature reach the equilibrium temperature slower at the thicker particle layer. Thus, to obtain faster drying, a thinner particle layer is necessary.

3.3. Effect of vapor temperature

Changes of evaporation flux, vapor temperature, and particle temperature versus time under different inlet vapor temperatures are shown in Fig.10-12. It is observed that the drying occurs faster at higher inlet vapor temperature. Hence, particles drying at lower inlet vapor temperature need longer time to reach the equilibrium moisture content. The maximum evaporate flux at $T_{v,in} = 240$ °C is 1.78 kg/m².s while at $T_{v,in} = 180$ °C, it is 1.18 kg/m².s. Vapor temperature (see Fig.11) drops to minimum temperature then increases gradually for every case, but at low inlet vapor temperature, the vapor temperature changes slower due to the slow heat and mass transfers (curve slope is small). Fig.12 shows the faster particle temperature change at higher inlet vapor temperature. Particularly, at $T_{v,in} = 240$ °C, the constant particle temperature as saturated temperature is remained for

100s while at $T_{v,in} = 180^\circ\text{C}$ it is remained for 160s. However, in all cases, heat transfer phenomena cease at almost the same time due to the differences between initial vapor temperature and particle temperature and the equilibrium values increase corresponding with the increase of inlet vapor temperature.

3.4. Effect of inlet vapor velocity

Evolutions of evaporation flux, vapor temperature and particle temperature at the middle

bed under different inlet vapor velocity are illustrated in Figs. 13-15.

The higher inlet velocity gives the increase in the heat and mass transfer flow rate between particles and vapor resulting in higher evaporation flux and shorter drying time. At $v_{v,in} = 2$ m/s, particle need 353s to stop evaporation while at $v_{v,in} = 1$ m/s, this period is 532s. Similarly, vapor temperature takes a longer time to reach the equilibrium temperature when the inlet vapor temperature is lower.

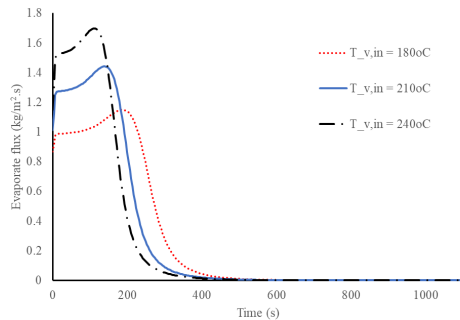


Fig. 10. Evaporation flux, m_v at the middle of the bed at $h = 0.1$ m, $v_{in} = 1.5$ m/s, $X_{w,in} = 0.2$ kg/kg, $d = 0.01$ m

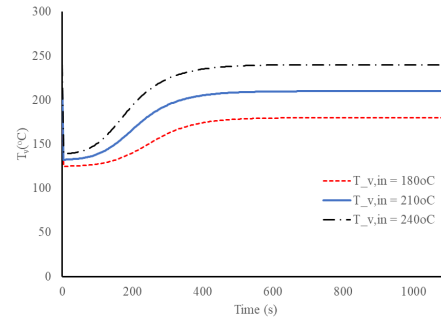


Fig. 11. Vapor temperature, T_v at the middle of the bed at $h = 0.1$ m, $v_{in} = 1.5$ m/s, $X_{w,in} = 0.2$ kg/kg, $d = 0.01$ m

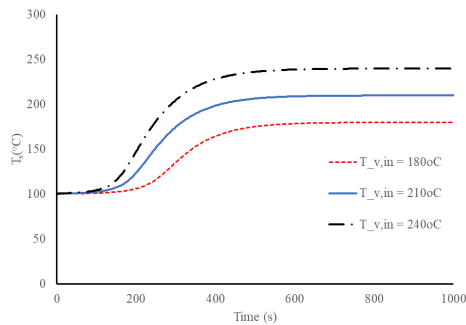


Fig. 12. Particle temperature, T_s at the middle of the bed at $h = 0.1$ m, $v_{in} = 1.5$ m/s, $X_{w,in} = 0.2$ kg/kg, $d = 0.01$ m

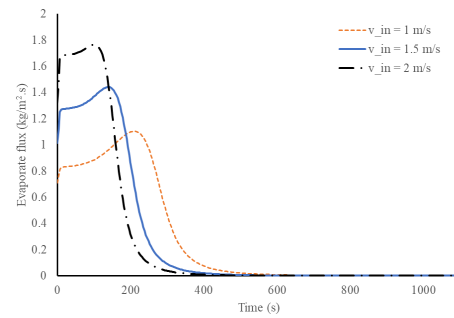


Fig. 13. Evaporation flux, m_v at the middle of the bed at $h = 0.1$ m, $T_{v,in} = 210$ m/s, $X_{w,in} = 0.2$ kg/kg, $d = 0.01$ m

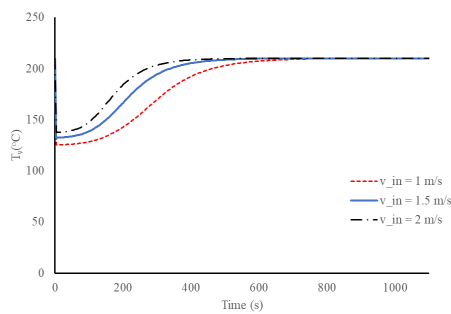


Fig. 14. Vapor temperature, T_v at the middle of the bed at $h = 0.1$ m, $T_{v,in} = 210^\circ\text{C}$, $X_{w,in} = 0.2$ kg/kg, $d = 0.01$ m

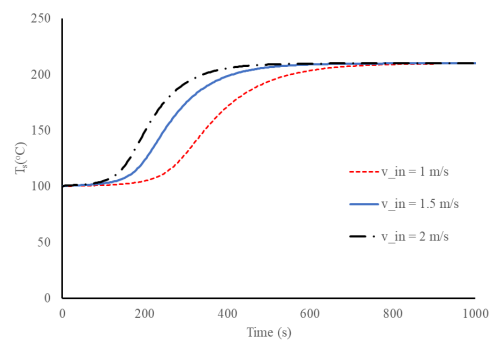


Fig. 15. Particle temperature, T_s at the middle of the bed at $h = 0.1$ m, $T_{v,in} = 210^\circ\text{C}$, $X_{w,in} = 0.2$ kg/kg, $d = 0.01$ m.

In Fig.14, vapor temperature drops suddenly to the minimum temperature then increases gradually to the equilibrium temperature (210°C). At $v_{v,in} = 1\text{m/s}$, vapor temperature is 210°C at 653 s while this temperature is 210°C at 420 s. The first drying period of particle is also longer at lower inlet vapor temperature so the constant particle temperature period at cooler drying is longer than hotter drying. After that, the particle temperature accelerates to the equilibrium temperature when heat transfer between particle and vapor stops at the almost same time with time vapor temperature ceases to change.

4. Conclusion

In this work, the impact of operating conditions on the super-heated steam drying by a packed bed of ceramic particles is analyzed based on the own published model. The results show that in order to accelerate evaporation, it is necessary to use the smaller particle, thinner bed layer, higher inlet vapor temperature, and faster inlet vapor velocity. Changes of drying data in the packed bed are different compared with drying kinetic of single particle. Under every condition, particles experience two drying periods: in the first period, evaporation flux increases to the maximum due to the change of vapor temperature resulting in the change of vapor physical properties, particle temperature remains as saturation temperature; in the second period, the evaporation flux reduces and particle temperature increases because of the fast increase in activation energy barrier.

This model can be implemented in the other dryers without any obstacle; however, it has several simplified assumptions, so the application ability is limited for the plug flow. If the partial gradient of vapor flow cannot be negligible, it is necessary to extend the developed model to the 3D model. In this case, the presented model should be combined with the momentum equation and the other equations which account for the effects of the dryer wall and pressure drop on the drying. In this case, the model computational fluid dynamic tool such as ANSYS Fluent or COMSOL Multiphysics which have many effective tools for complex mathematical models. That is also the next step of authors' project.

Acknowledgments

This research is funded by Vietnam National Foundation for Science and Technology

Development (NAFOSTED) under grant number 107.99-2018.06.

References

- [1]. Mujumdar, A.S. Handbook of industrial drying; CRC Press: Boca Raton, 2014.
- [2]. Romdhana, H.; Bonazzi, C.; Esteban-Decloux, M. Superheated Steam Drying: An Overview of Pilot and Industrial Dryers with a Focus on Energy Efficiency. *Drying Technology* 2015, 33(10), 1255–1274.
- [3]. Zhu, J.; Wang, Q.; Lu, X. Status and Developments of Drying Low Rank Coal with Superheated Steam in China. *Drying Technology* 2015, 33(9), 1086–1100.
- [4]. Prado, M.M.; Mazzini Sartori, D.J. Heat and Mass Transfer in Packed Bed Drying of Shrinking Particles. In *Mass transfer in multiphase systems and its applications*; El-Amin, M., Ed.; InTech: Rijeka, 2011.
- [5]. Adamski, R.; Pakowski, Z. Identification of Effective Diffusivities in Anisotropic Material of Pine Wood during Drying with Superheated Steam. *Drying Technology* 2013, 31(3), 264–268.
- [6]. Pakowski, Z.; Adamski, R.; Kwapisz, S. Effective diffusivity of moisture in low rank coal during superheated steam drying at atmospheric pressure. *Chemical and Process Engineering* 2012, 33(1), 43–51.
- [7]. Ezhil, C. Superheated steam drying of foods-A review. *World journal of dairy and food sciences* 2010, 5(2), 214–217.
- [8]. Sehrawat, R.; Nema, P.K.; Kaur, B.P. Effect of superheated steam drying on properties of foodstuffs and kinetic modeling. *Innovative Food Science & Emerging Technologies* 2016, 34, 285–301.
- [9]. Messai, S.; El Ganaoui, M.; Sghaier, J.; Chrusciel, L.; Slimane, G. Comparison of 1D and 2D models predicting a packed bed drying. *International Journal for Simulation and Multidisciplinary Design Optimization* 2014, 5(10), A14.
- [10]. Le, K.H.; Tran, T.T.H.; Nguyen, N. an; Kharaghani, A. Multiscale modelling of superheated steam drying of particulate materials. *Chemical Engineering & Technology* 2020.
- [11]. Hager, J.; Wimmerstedt, R.; Whitaker, S. Steam drying a bed of porous spheres: Theory and experiment. *Chemical Engineering Science* 2000, 55(9), 1675–1698.